# A RANSAC based phase noise filtering method for the camera-projector calibration system*

**LI Wenjie[1], ZHANG Zonghui[1], JIANG Zhansi[1], GAO Xingyu[1], TAN Zhengdong[2], and WANG Hui[3]****

*1. School of Mechanical and Electrical Engineering, Guilin University of Electronic Technology, Guilin 541004, China*

*2. Shenzhen Anewbest Electronic Technology Limited Company, Shenzhen 518000, China*

*3. Communist Youth League Committee, Guilin University of Electronic Technology, Guilin 541004, China*

(Received 27 March 2022; Revised 15 May 2022)



Aiming at the noise disturbance of unwrapping phases of control points in the camera-projector calibration system, a random sample consensus (RANSAC) based plane fitting method is proposed to filter the phase noise in this paper. Different from the classical least squares method using all data, the points with noise will not be used to fit the plane in the proposed RANSAC method, which improves the accuracy of plane fitting. The proposed method suits for any two-dimensional (2D) calibration patterns, such as checkerboard or black dots with white background, which improves the flexibility of camera-projector system calibration.

**Document code:** A **Article ID:** 1673-1905(2022)10-0618-5

**DOI** https://doi.org/10.1007/s11801-022-2045-2

As the important tool, three-dimensional (3D) imaging technology is one of the hot researches in the fields of calculation imaging and geometric measurement[1-3]. With the advantages of non-contact, quick and high accuracy, optics based 3D technology is popular in the fields of daily consumption and industrial detection[4,5]. Among them, the fringe projection profilometry (FPP) system with single camera and projector is used widely in industrial inspection, benefitting from the simple structure, quick imaging and so on[6-8]. The main principle is that the standard fringe patterns from projector are modulated as the deformed fringe patterns by the measured surface, and they are acquired by camera. Phase recovery algorithm is performed to obtain the phase map. Combining with the system parameters, the surface profiles are reconstructed. Therefore, the system calibration is the key part for 3D reconstruction[9]. In the FPP system, calibration can be divided into model based, polynomial based and least square based ones[10]. ZHANG et al[11] calibrated simply and quickly the FPP system using the relationship between the unwrapping phases (UPs) and camera coordinate. The pixel coordinates and UPs of control points with high accuracy are needed in this model. The sub pixel coordinates are got based on the control points extraction method, and the neighborhood UPs interpolation algorithm is performed to get the fine UPs of control points. Although the accuracy of UPs is improved based on the multi-frequency heterodyne method in theory[12], the UPs of control points suffered from the neighborhood phase noise easily[13]. To ensure the UPs accuracy of neighborhood points, the specific calibrators such as white circular dots with black background or circular rings with white background are usually used in the system calibration, while the common calibrators such as checkerboard or black dots with white background are not accepted, which limits the application and universality of system calibration.

In this paper, a flexible system calibration method for the camera-projector system is proposed, which suits for any two-dimensional (2D) calibration patterns including checkerboard. In the proposed method, the random sample consensus (RANSAC) based plane fitting is used to constrain the coplanarity of UPs of control points and the UPs with noise are filtered effectively.

The camera-projector calibration system model is shown in Fig.1, including camera coordinates, pixel coordinates and UPs, and the mapping relation of point $P$ is established. According to the similarity between triangles, $\Delta OP'P''\cong\Delta OD'D''$, $\Delta DP'P\cong\Delta DOO_p$, we have

$$\begin{cases}\dfrac{OP''}{OD''}=\dfrac{OP'}{OD}\\ \dfrac{DP'}{OD}=\dfrac{PP'}{OO_p}\end{cases},\tag{1}$$

and then we have

$$\frac{OP''}{OD''}=\frac{OO_p-PP'}{OO_p}.\tag{2}$$

* This work has been supported by the Guangxi Science and Technology Base and Special Talents Program (No.2018AD19077), the Guangxi Innovation and Driving Development Special Funds Project (No.AA18118002-3), and the Guangxi Natural Science Foundation (No.2018JA170110).

** E-mail: 283770104@qq.com

If the world coordinate of point $P$ is ($X_w$, $Y_w$, $Z_w$), then $OP''=X_w$, $PP'=Z_w$. Commanding $OO_p=l$.

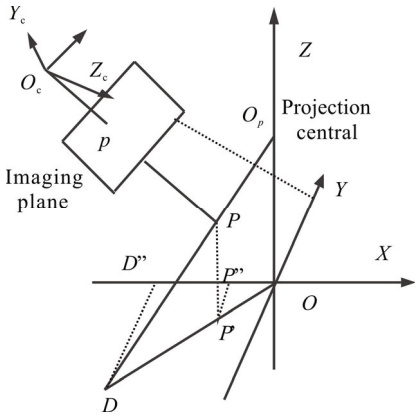


**Fig.1 System calibration principle**

Combining the fringe projection, we have

$$OD'' = \frac{\lambda_0}{2\pi}(\theta - \theta_0), \tag{3}$$

where $\lambda_0$ is the fringe period, and $\theta$ and $\theta_0$ are the UPs and reference phases, respectively. Combining Eqs.(2) and (3), the relation between the world coordinate and unwrapping phase of point $P$ is

$$\theta = \frac{(2\pi l / \lambda_0)X_w - \theta_0 Z_w + l\theta_0}{l - Z_w}. \tag{4}$$

Then, the relation between the camera coordinate and UP of point $P$ is

$$\theta = \frac{a_1 X_c + a_2 Y_c + a_3 Z_c + a_4}{a_5 X_c + a_6 Y_c + a_7 Z_c + a_8}, \tag{5}$$

where $a_1$, $a_2$, …$a_8$ are system parameters, and ($X_c$, $Y_c$, $Z_c$) is the camera coordinate of point $P$. The relationship between the pixel and camera coordinates is[14]

$$\rho\begin{bmatrix} u \\ v \\ 1 \end{bmatrix} = \begin{bmatrix} f_x & 0 & u_0 & 0 \\ 0 & f_y & v_0 & 0 \\ 0 & 0 & 1 & 0 \end{bmatrix}\begin{bmatrix} X_c \\ Y_c \\ Z_c \end{bmatrix} = \boldsymbol{M}\begin{bmatrix} X_c \\ Y_c \\ Z_c \end{bmatrix}, \tag{6}$$

where ($u$, $v$) is the pixel coordinate after the distortion correction, ($u_0$, $v_0$) is the principal point, and $\boldsymbol{M}$ is the internal parameter matrix. The $f_x$ and $f_y$ are the focal lengths. According to Eqs.(5) and (6), ($X_c$, $Y_c$, $Z_c$) of point $P$ can be calculated using the pixel coordinate and unwrapping phase after the system calibration. The flow chart of system calibration is presented in Fig.2.

The images of calibrator and responding fringe projection at different positions are acquired. The camera calibration is performed to get the $\boldsymbol{M}$ and $\boldsymbol{RT}$, and control point ($X_c$, $Y_c$, $Z_c$) is calculated according the world coordinate. The wrapping phases are calculated based on the least squares method[15]

$$\Phi = \arctan\left(\frac{-\sum_{i=1}^{N} I_i \sin(\delta_i)}{\sum_{i=1}^{N} I_i \cos(\delta_i)}\right), \tag{7}$$

where $I_i$ and $\delta_i$ are the intensity distribution and phase shift at the $i$th fringe pattern. The three frequencies heterodyne method is used to get the UPs, and interpolation algorithm is used to get UPs of control points. Singular value decomposition (SVD) is performed to get the system parameters ($a_1$, $a_2$…$a_8$). So the high accuracy of pixel coordinates and UPs of the control points is important to the system calibration.

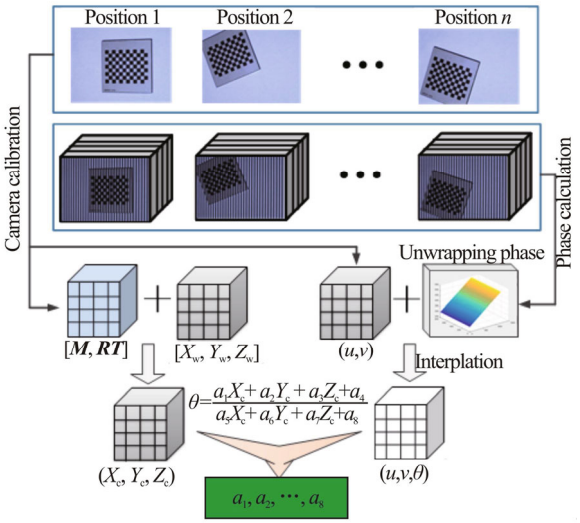


**Fig.2 Flow chart of system calibration**

The control points on the calibrators are coplanar, so the UPs of control points are also constrained by the coplanarity in theory. To avoid the system calibration result sufferring from the phase noise, the coplanarity constrain of UPs is used to filter the UPs noise of control points. The methods of plane fitting include least squares based method and the RANSAC based method.

The least squares based plane fitting method takes all data ($x_i$, $y_i$, $z_i$) ($i$=1, 2…$N$) to fit the plane. The fitting condition is the minimum sum of squares of distances from all points to the fitting plane, shown as

$$S = \sum_{i=1}^{N}(ax_i + by_i + c - z_i)^2, \tag{8}$$

where $a$, $b$, $c$ are the coefficients of fitting plane. They will be calculated using the least squares algorithm as

$$\begin{cases} \dfrac{\partial S}{\partial a} = \sum_{i=1}^{N} 2x_i(ax_i + by_i + c - z_i) = 0 \\ \dfrac{\partial S}{\partial b} = \sum_{i=1}^{N} 2y_i(ax_i + by_i + c - z_i) = 0 \\ \dfrac{\partial S}{\partial c} = \sum_{i=1}^{N} 2(ax_i + by_i + c - z_i) = 0 \end{cases}. \tag{9}$$

In this method, all points are used to fit the plane, including the points with noise. The fitting result will be suffered from the noise.

Using the iteration algorithm, RANSAC estimates the

model parameters from a group of data including both the correct and abnormal data. The correct data is labeled as inliers and the abnormal data is labeled as outliers. The features of the algorithm are randomness and hypothesis. The sample data is selected randomly according to the probability of the occurrence of correct data. The hypothesis is to assume that the selected sample data are all correct, and then using them to record the number of other points as inliers. Under the same criterion, the model parameters with the most inliers are the results we need. Compared with the least square method, the outliers are not used to calculate the model parameters in the RANSAC method, which can get a higher precision result. The flow of RANSAC based plane fitting is shown in Fig.3.

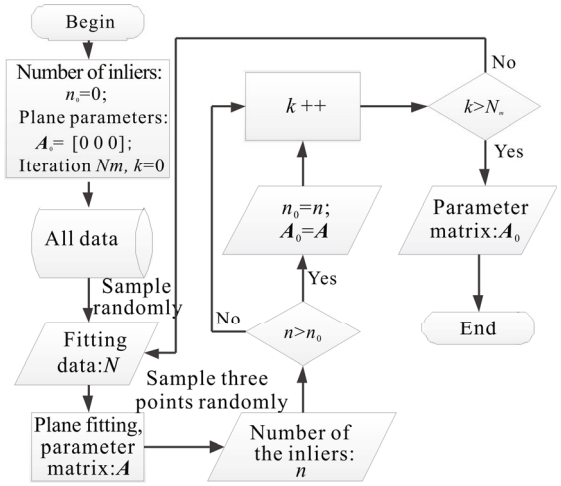


**Fig.3 Flow of the RANSAC based plane fitting**

The main steps are as follows.

(1) Sample three points randomly from the fitting data to fit a plane.

(2) Calculate the distances of all fitting data to the fitting plane.

(3) Record the number of inliers according the distance threshold.

(4) Repeat the steps (1)—(3), until the iteration is end. Then the fitting plane that has the most inliers is the required plane.

In the UP map of calibrator, the majority points are coplanar. So the real plane including the control points will be found using the RANSAC based plane fitting, as long as the iteration is enough.

According to the pixel coordinates and the real UP map, the phases of control points are got based on the interpolation method. The distance of UP point ($x_i$, $y_i$, $z_i$) to the fitting plane can be denoted as

$$d_i = (ax_i + by_i + c - z_i)^2, \tag{10}$$

where $A$=[$a$ $b$ $c$] is the coefficient matrix. If the distance threshold is $d_T$, the estimation criteria of inliers is

$$\begin{cases} d > d_T, & \text{outliers} \\ d < d_T, & \text{inliers} \end{cases}. \tag{11}$$

To verify the efficiency and feasibility, a camera-projector system was set up, and the system calibration was performed using the checkerboard. The parts of parameters of camera and projector are presented in Tab.1. The images of checkerboard and fringe pattern are captured at different positions. Camera calibration was performed to get the pixel coordinates of control points, internal parameter matrix ***M*** and external parameter matrix ***RT***. The four step phase shift and three frequencies heterodyne method are used to get the unwrapping phase. The three frequencies are [70 64 59]. Then the Ups of control points were got by the interpolation algorithm.

**Tab.1 Parameters of camera and projector**

| | Company | Context |
|---|---|---|
| Camera | MV | 1 200 pixel×1 600 pixel |
| Projector | TI | Dlp4500 |

The diagrams of fringe pattern and UP map are shown in Fig.4. There are many points with noise in the UP map. The sine property of fringe pattern is bad in the black areas of the checkerboard.

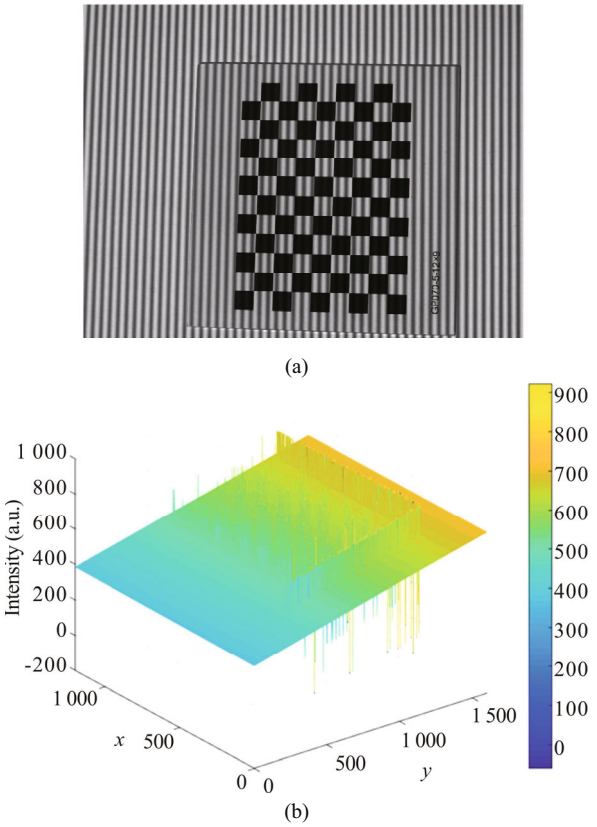


**Fig.4 Diagrams of (a) fringe pattern and (b) unwrapping phase**

To verify the necessary of noise filtering, the UPs of control points are extracted directly, and the coplanarity is analyzed using the least squares and RANSAC methods respectively. As shown in Fig.5, the distance threshold $d_T$ is 0.5 rad. The inliers and outliers are denoted by "×" and "O" respectively. As shown in Fig.5(a), the least squares based plane fitting method suffers from the UP with noise and many phases of control points are classified as outliers. While the RANSAC based plane fitting method is not sensitive to the UP with noise, and the many phases of control points are classified as inliers. The comparison experiment shows the proposed UP noise filtering method is efficient.

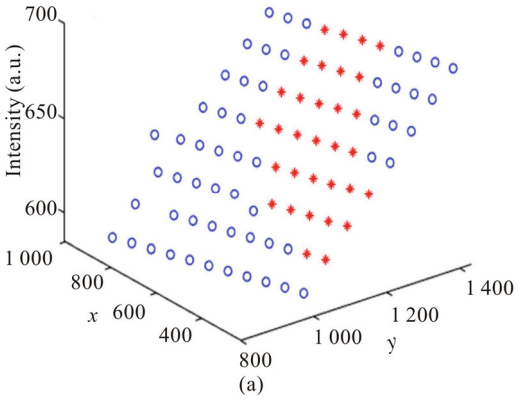


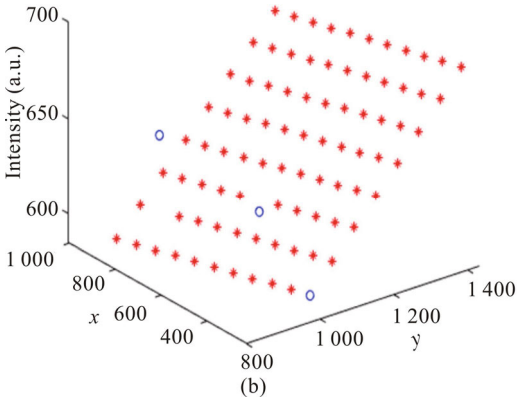


**Fig.5 Unwrapping phase maps comparison using (a) least squares method and (b) RANSAC method**

In order to prove the necessity of de-noise for phase, two group of data sets were used to calculate the calibration parameters in the experiment. Group *A* does not take the phase noise into condition, and extracts the UPs of control points directly. Group B uses the proposed RANSAC based plane fitting to filter the UPs of control points with noise. The system parameters can be calculated by Eq.(5), and the results are shown in Tab.2.

**Tab.2 Calibration parameters**

| | $a_1$ ($\times 10^{-1}$) | $a_2$ ($\times 10^{-4}$) | $a_3$ ($\times 10^{-3}$) | $a_4$ | $a_5$ ($\times 10^{-6}$) | $a_6$ ($\times 10^{-6}$) | $a_7$ ($\times 10^{-5}$) | $a_8$ ($\times 10^{-4}$) |
|---|---|---|---|---|---|---|---|---|
| *A** | −1.21 | −7.20 | −3.00 | −1.00 | −1.92 | −1.63 | −1.02 | 3.47 |
| *B** | −1.31 | −8.50 | −3.40 | −1.00 | −1.19 | −1.82 | −1.15 | 5.44 |

**A* and *B* are the calibration results with denoising and without denoising, respectively.

To verify the accuracy of the calculated system parameters, the corners information ($u$, $v$, $\theta$) of seven checkerboard patterns at different positions were used to back calculate their camera coordinates. The real distance of adjacent corners is 5 mm. One of the distance map comparison is shown in Fig.6, and the results with and without the noise filtering are presented by "×" and "O" respectively. Obviously, the proposed method with phase noise filtering can get a better result. Their root mean square errors (*RMSE*) comparison is shown in Tab.3. *A* and *B* are the results without and with UP noise filtering to the control points respectively. With UP noise filtering, the data fluctuation is improved, which agrees with the theory analysis, and indicates the UP noise filtering to the control points is necessary.

In this paper, an RANSAC based UP of control points noise filtering method is proposed in the camera-projector system calibration. The UP noise of control points is filtered efficiently, and system calibration result is improved. The proposed method suits for any 2D calibration patterns, such as checkerboard, black dots with white background, which improves the flexibility of the system calibration.

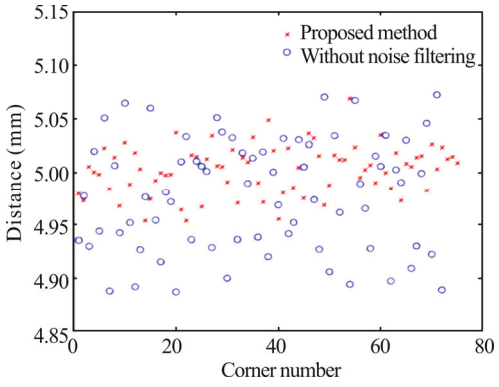


**Fig.6 Adjacent corners distance comparison**

**Tab.3 Distance *RMSE* comparison**

| Patterns | 1 | 2 | 3 | 4 | 5 | 6 | 7 |
|---|---|---|---|---|---|---|---|
| *A* | 8.4 | 5.7 | 4.3 | 12.8 | 11.6 | 15.7 | 23 |
| *B* | 23.3 | 16.4 | 17.2 | 36.4 | 27.0 | 37.8 | 59 |

When the phase noise is large, the advantage of proposed method is obvious compared with the least squares method. Because of the randomness and hypothesis in the RANSAC method, the proposed method needs enough iteration, which is time consuming compared with the least square method. In the proposed method, adaptively getting the distance threshold is important, which is our next interesting work.

## Statements and Declarations

The authors declare that there are no conflicts of interest related to this article.

## References

[1] HUANG C, HUANG Y, CHAN D, et al. Shape-reserved stereo matching with segment-based cost aggregation and dual-path refinement[J]. EURASIP journal on image and video processing, 2020, 2020(38).

[2] HU Y, LIANG Z, FENG S, et al. Calibration and rectification of bi-telecentric lenses in Scheimpflug condition[J]. Optics and lasers in engineering, 2022, 149：106793.

[3] FENG S, ZUO C, ZHANG L, et al. Calibration of fringe projection profilometry：a comparative review[J]. Optics and lasers in engineering, 2021, 143：106622.

[4] LI W, ZHANG Q, ZHONG L, et al. Image definition assessment based on Tchebichef moments for micro-imaging[J]. Optics express, 2019, 27(24)：34888.

[5] JI Y, CHEN Y, SONG L, et al. 3D defect detection of connectors based on structured light[J]. Optoelectronics letters, 2021, 17(2)：107-111.

[6] SURESH V, HOLTON J, LI B. Structured light system calibration with unidirectional fringe patterns[J]. Optics and lasers in engineering, 2018, 106：86-93.

[7] KANG X, LI T, SIA B, et al. A novel calibration method for arbitrary fringe projection profilometry system[J]. Optik - international journal for light and electron optics, 2017, 148：227-237.

[8] SONG L, LIN W, YANG Y, et al. Fast 3D reconstruction of dental cast model based on structured light[J]. Optoelectronics letters, 2018, 14(6)：457-460.

[9] SONG L, CHEN C, CHEN Z, et al. Essential parameter calibration for the 3D scanner with only single camera and projector[J]. Optoelectronics letters, 2013, 9(2)：143-147.

[10] ZHANG Z, MA H, ZHANG S, et al. Simple calibration of a phase-based 3D imaging system based on uneven fringe projection[J]. Optics letters, 2011, 36(5)：627-629.

[11] ZHANG Z, HUANG S, MENG S, et al. A simple, flexible and automatic 3D calibration method for a phase calculation-based fringe projection imaging system[J]. Optics express, 2013, 21(10)：12218.

[12] DI DONATO A, FABI G, MENCARELLI D, et al. Heterodyne phase shifting method in scanning probe microscopy[J]. Journal of the Optical Society of America A, optics, image science, and vision, 2021, 38(3)：378-386.

[13] XUE Q, JI W, MENG H, et al. Estimating the quality of stripe in structured light 3D measurement[J]. Optoelectronics letters, 2022, 18(2)：103-108.

[14] ZHANG Z. A flexible new technique for camera calibration[J]. IEEE transactions on pattern analysis and machine intelligence, 2000, 22(11)：1330-1334.

[15] MUÑOZ A, FLORES J L, PARRAESCAMILLA G, et al. Least-squares gamma estimation in fringe projection profilometry[J]. Applied optics, 2021, 60(5)：1137.